American Mineralogist, Volume 66, pages 260–277, 1981

A thermodynamic model of mineral segregations in the lower sillimanite zone near Rangeley, Maine

C. T. FOSTER, JR.

Department of Geology, The University of Iowa
Iowa City, Iowa 52242

Abstract

A local equilibrium, irreversible thermodynamic approach is used to model metamorphic segregations in pelites from the lower sillimanite zone near Rangeley, Maine. Relative phenomenological coefficients for the model are derived from a reaction involving sillimanite and another reaction involving staurolite using a least-squares technique to give the best fit to the observed data. The mean values of the relative coefficients in an SiO_2 fixed (= inert marker?) reference frame from five rocks in the middle of the lower sillimanite zone are: $AlO_{1.5} = 5.9$, $FeO = 2.6$, $MgO = 1.8$, $KO_{0.5} = 1.0$, $NaO_{0.5} = 0.9$, $TiO_2 = 0.4$, and $CaO = 0.2$. The phenomenological coefficients are used with Gibbs–Duhem relations and conservation equations to give the sequence of mantles, mineral modes in each mantle, chemical potential profiles, and size of segregations that are expected to form around reacting sillimanite, staurolite, and garnet. The model predicts that: sillimanite growth will produce a segregation with a muscovite-free, biotite-rich mantle surrounding a sillimanite- and quartz-rich core; staurolite will be replaced by a muscovite-rich pseudomorph; and matrix garnets should be rimmed by thin biotite-free mantles. Comparison of the computed textures with those observed in the rocks shows a good match except for the case of garnet, where new garnet growth was not sufficient to produce well-defined mantles in the relatively coarse-grained matrix.

Introduction

Cation-exchange reaction mechanisms are commonly invoked by petrologists to reconcile complex metamorphic textures with isograd reactions inferred from field relations (*e.g.* Foster, 1977a; Hollister, 1977; Yardley, 1977; Bailes and McRitchie, 1978). These mechanisms involve several local reactions in different microscopic domains of the rock which communicate with each other *via* the migration of components from one region to another (Carmichael, 1969). Some workers (Eugster, 1970; Fisher, 1970; Olsen, 1972; Foster, 1975) have investigated metamorphic processes of this kind using a graphical approach to show that local chemical potential gradients of some components are in the proper direction to account for the required material transport from one domain to another. However, it is difficult to use these methods to examine chemical potential gradients of more than a few components and to quantify the relative rates of transport and reaction which occur in different parts of a rock. Consequently, more elaborate analytical approaches have been developed using irreversible thermodynamics to evaluate gradients, fluxes, and reaction rates in metamorphic rocks (Fisher, 1973, 1975, 1977; Frantz and Mao, 1976, 1979; Loomis, 1976; Weare *et al.*, 1976).

This paper uses irreversible thermodynamics to construct a quantitative model of reactions which formed mineral segregations in pelites from the lower sillimanite zone on Elephant Mountain near Rangeley, Maine. Foster (1977a) found that three types of mineral segregations were formed by reactions in these rocks as grade increased within the zone: (1) a sillimanite segregation composed of a sillimanite-rich core and a muscovite-free mantle; (2) a staurolite segregation composed of a staurolite poikiloblast surrounded by a coarse, mica-rich rim; and (3) a garnet segregation consisting of a garnet porphyroblast set in a matrix of muscovite, biotite, plagioclase, quartz, and ilmenite. The development of these segregations was attributed to the cation-exchange reaction mechanism shown in Figure 1. The reaction begins when sillimanite nucleates and grows in a biotite, muscovite, plagioclase, quartz, ilmenite matrix which surrounds garnet and staurolite porphyroblasts. The net local reaction in this segregation primarily consumes muscovite and plagioclase while producing sil-

0003–004X/81/0304–0260$02.00

limanite and biotite. As the sillimanite segregation grows, staurolite surrounded by matrix in another domain of the rock dissolves. It is replaced by a pseudomorph that is dominated by muscovite with lesser amounts of biotite, plagioclase, quartz, and ilmenite. Garnets surrounded by matrix also grow a small amount during the reaction. When the local reactions in the rock are summed together they equal the continuous reaction inferred from field relations (Guidotti, 1970, 1974; Foster, 1977a).

Fundamental relationships

Rate and conservation equations

The cation exchange reaction shown in Figure 1 involves two basic types of phenomena: (1) chemical reactions and (2) the transport of material between reaction sites. A quantitative model of this reaction mechanism must analytically relate the rates of reaction and material transport at any particular point in the rock to the forces which drive the reactions and material transfer. This can be accomplished through equations commonly used to describe irreversible thermodynamic processes (DeGroot and Mazur, 1962; Katchalsky and Curran, 1965). The approach used in this paper is derived from Fisher (1973, 1975, 1977).

The magnitude and direction of flow of components at any particular point may be related to chemical potential gradients at that point by the set of equations:

$$J_i = -\sum_{j=1}^{n} L_{ij} \nabla \mu_j \qquad (i=1,2,\ldots,n) \qquad (1)$$

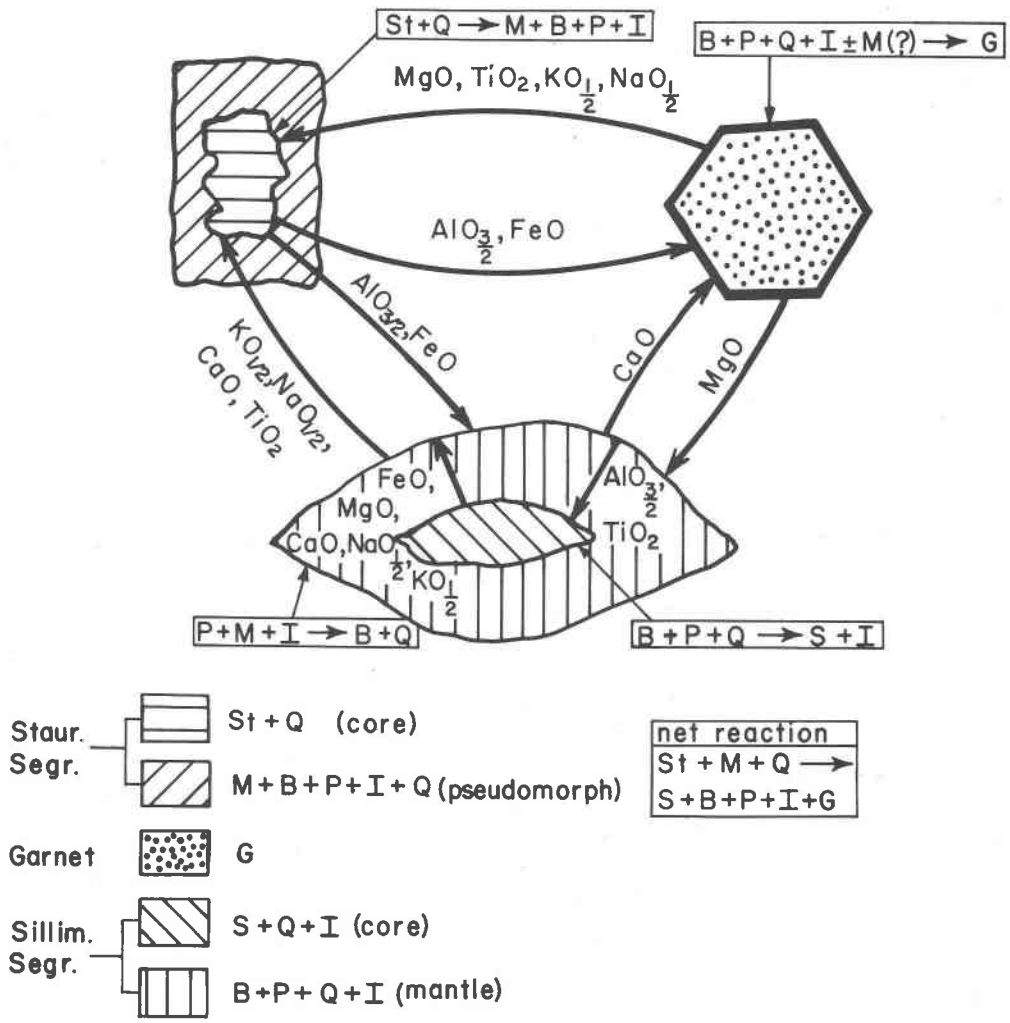

Fig. 1. Cation exchange reaction mechanism for sillimanite-bearing rocks near Rangeley, Maine. St = staurolite, S = sillimanite, G = garnet, B = biotite, M = muscovite, P = plagioclase, I = ilmenite, Q = quartz.

where J_i is the flux of component i, $\nabla\mu_j$ is the chemical potential gradient of component j, L_{ij} is the diffusion phenomenological coefficient which relates the flux of component i to the chemical potential gradient of component j, and n is the number of components. The rate of chemical reactions at any point is given by a similar set of equations:

$$J_k^r = \sum_{m=1}^{q} L_{km}^r A_m \qquad (k=1,2,\ldots,q) \qquad (2)$$

where J_k^r is the rate of reaction k, A_m is the affinity of reaction m, L_{km}^r are reaction phenomenological coefficients which relate the rate of reaction k to the affinity of reaction m, and q is the number of reactions in the system. The affinity of a reaction is a measure of how far the reaction is from equilibrium. It is given by the relation:

$$A_m = -\sum_{i=1}^{n} \nu_{im}\Delta\mu_i \qquad (=0 \text{ at equilibrium}) \qquad (3)$$

where ν_{im} is the stoichiometric coefficient of component i in reaction m and $\Delta\mu_i$ is the difference between the equilibrium value of μ_i and the actual value of μ_i. If a system is composed of solids surrounded by a fluid the transport of material in the fluid is related to reactions between the solids and the fluid by a conservation equation:

$$\partial c_i/\partial t + \nabla \cdot J_i = \sum_{k=1}^{p} \nu_{ik} J_k^r \qquad (4)$$

where c_i is the concentration of component i in the fluid at the point of interest, $\nabla \cdot J_i$ is the divergence of component i at the point of interest and $\Sigma_{k=1}^{p} \nu_{ik} J_k^r$ is the rate of production of component i by p chemical reactions at the point of interest. The reactions in equation 4 can be chosen to be those that represent the precipitation of individual minerals from components dissolved in the fluid phase. Under this convention, J_k^r gives the rate of precipitation of mineral k at the point of interest. When $J_k^r > 0$ mineral k precipitates from the fluid. When $J_k^r < 0$ mineral k dissolves in the fluid.

Equation 4 can be integrated over a volume V to give the total production of component i by chemical reactions taking place within the volume:

$$\int_V \left(\sum_{k=1}^{p} \nu_{ik} J_k^r \right) dV = \int_V \partial c_i/\partial t \, dV + \int_V (\nabla \cdot J_i) \, dV \qquad (5)$$

in which $\int_V$ denotes the volume integral. The volume integral of the divergence of component i is related to the integral of the flux of i over the surface surrounding the volume by the divergence theorem (Sokolnikoff and Redheffer, 1966, p. 397–398):

$$\int_V (\nabla \cdot J_i) \, dV = \int_s J_i \cdot dA \qquad (6)$$

in which $\int_s$ denotes the integral over the surface which surrounds the volume V. Substitution in equation 5 using equation 6 gives:

$$\int_V \left(\sum_{k=1}^{p} \nu_{ik} J_k^r \right) dV = \int_V \partial c_i/\partial t \, dV + \int_s J_i \cdot dA \qquad (7)$$

which provides a relation between the production of component i by chemical reactions within a volume (given by the first term of the equation) and the transport of component i into or out of the volume (given by the last term of the equation). The middle term in equation 7 represents a source or sink for component i which is present if the concentration of component i in the fluid contained in the volume V changes as the reactions proceed. In the Rangeley rocks this term is probably very small when compared to the other terms because the volume of fluid present along the grain boundaries in the rock is several orders of magnitude less than the volume of minerals produced by reactions in the segregation. In addition, the concentration gradients between the segregations are believed to be small because: (1) microprobe analyses suggest that pelites throughout the lower sillimanite zone are fairly well equilibrated (Guidotti, 1970, 1974), (2) the sillimanite-forming reaction was never overstepped by a large amount because sillimanite preferentially nucleates only in biotite (Foster, 1975, 1977a), and (3) the overall reaction within the lower sillimanite zone is a continuous reaction (Guidotti, 1970, 1974), so the entire rock would be expected to be at or near equilibrium over a range of temperatures and pressures. When the middle integral in equation 7 is negligible the equation simplifies to:

$$\int_V \left(\sum_{k=1}^{p} \nu_{ik} J_k^r \right) dV = \int_s J_i \cdot dA \qquad (8)$$

which states that the amount of component i used or consumed by the sum of the reactions occurring within the volume V must be supplied or removed by material transport between the volume V and its surroundings.

Local equilibrium and reaction rates

Two types of rates are related by equation 8: the rate of reaction and the rate of material transport.

These rates are related to the chemical potentials of components by equations 2 and 1. If the rate of reaction is slow relative to the rate of material transport the affinity of the reaction (*i.e.*, the difference between the equilibrium and actual values of the chemical potentials) will be large relative to the chemical potential gradients in the rock. Segregations which grow under conditions such as these are said to be reaction controlled. On the other hand, if the rate of reaction is fast relative to the rate of material transport the affinity of the reactions in the rock will be small when compared to the chemical potential gradients and reactions will occur near equilibrium. If bulk flow of material through the rock is not occurring then reactions taking place in the rock are governed by chemical potential gradients which cause diffusion to transport material from one area of the rock to another. Reactions of this type are called diffusion controlled. Calculations by Fisher (1977) suggest that reactions in segregations of the type reported by Foster (1977a) should be controlled by diffusion of material along grain boundaries. The shape of segregations in these rocks also supports a diffusion-controlled reaction mechanism because the segregations, which are post-tectonic, tend to be elongate in the direction which has the largest number of grain boundaries. This suggests that the rate of the reaction which forms a segregation depends upon the number of grain boundaries through which material can be supplied, as would be expected in a diffusion-controlled reaction (Foster, 1976; Fisher, 1977).

Because reactions are relatively fast in diffusion-controlled processes, any significant deviation from equilibrium caused by material transport will be immediately countered by a reaction that will keep the system in a state which is relatively close to equilibrium. In these circumstances the chemical potentials at a point along the grain boundaries in the rock will be essentially in equilibrium with the local mineral assemblage. A system which behaves in this way is said to be in local equilibrium (DeGroot and Mazur, 1962; Katchalsky and Curran, 1965; Korzhinskii, 1959; Thompson, 1959). If a system is in local equilibrium the chemical potential gradients at any point are governed by the Gibbs–Duhem relations of the phases present so that:

$$\sum_{j=1}^{n} \nu_j^k \nabla\mu_j = 0 \qquad (k=1,2,\ldots,p) \tag{9}$$

where ν_j^k is the stoichiometric coefficient of component j in phase k, $\nabla\mu_j$ is the chemical potential gradient of component j, n is the number of components and p is the number of phases present at the point.

Calculation of local reactions

The local reactions which take place in metamorphic rocks depend upon the composition of the phases present, reaction rates, and the ability of components to move towards or away from a reaction interface. The type of local reaction of interest in this paper involves one mineral growing or dissolving in a homogeneous matrix of other minerals under local equilibrium conditions. An example of this type of reaction is the nucleation and growth of sillimanite in a matrix of muscovite, biotite, plagioclase, quartz, and ilmenite which formed the sillimanite segregations in Figure 1. If the grain boundary phase does not act as a net source or sink of material, then the components produced or consumed by the reaction between the core mineral and matrix minerals must be supplied or removed by diffusion down chemical potential gradients in the matrix surrounding the core mineral. This is expressed mathematically by substituting for the flux terms (J_i) in equation 8 using equation 1:

$$\int_V \left(\sum_{k=1}^{p} \nu_{ik} J_k^r\right) dV = \int_s \left(-\sum_{j=1}^{n} L_{ij} \nabla\mu_j\right) \cdot dA \qquad (i=1,2,\ldots,n) \tag{10}$$

The right-hand integral represents the net amount of component i which passes through a closed surface in the matrix which surrounds the segregation during its growth. The left-hand integral represents the net amount of component i consumed by all of the reactions taking place within the volume enclosed by the surface. Because the segregations to be modelled are approximately spherical, the surface surrounding the segregation has been chosen to be a sphere with its center positioned at the center of the segregation. An additional simplifying assumption is that the chemical potential gradients and reactions are constant at all points equidistant from the center of the sphere. This allows equation 10 to be simplified to

$$4\pi \int_0^x \left(\sum_{k=1}^{p} \nu_{ik} J_k^r\right) x^2\, dx = -4\pi x^2 \sum_{j=1}^{n} L_{ij} (\nabla\mu_j)_x \qquad (i=1,2,\ldots,n) \tag{11}$$

where x represents the radius of the spherical surface surrounding the segregation and $(\nabla\mu_j)_x$ is the chemical potential gradient of component j evaluated at a distance x from the center of the segregation.

Provided that local equilibrium is maintained, the chemical potential gradients in equation 11 are constrained by the Gibbs–Duhem relations (equation 9) of the phases surrounding the segregation. Thus, for an n-component system in which a new phase is growing at the expense of p − 1 matrix phases there are p + n unknowns: n chemical potential gradients in the matrix at the surface of the sphere which surrounds the reacting phases and p reaction coefficients describing the net reaction that takes place within the sphere when the new mineral grows at the expense of the matrix minerals. There are a total of n + p − 1 equations that constrain the system: n conservation equations like equation 11 (one for each component) and p − 1 Gibbs–Duhem relations (one for each matrix mineral). If the value of one of the unknowns can be estimated, then the system is constrained by an additional equation that sets the value for the estimated unknown. Then, the p + n equations can be solved simultaneously for p + n unknowns (Fisher, 1975, 1977). Unfortunately, in most geologic systems neither the chemical potential gradients nor any of the reaction rates are known. In this case, the relative chemical potential gradients and the relative reaction rates can be obtained by solving the matrix equation given in Figure 2. The first p − 1 equations in Figure 2 can be obtained by multiplying the Gibbs–Duhem relations (equation 9) by a constant (A/R_p) giving it the form:

$$\sum_{j=1}^{n} \nu_j^k (\nabla\mu_j)_x \cdot (A/R_p) = 0 \qquad (k=1,2,\ldots,p-1) \qquad (12)$$

where A is the surface area of the sphere of radius x where the chemical potential gradients are measured and R_p is the net amount of phase p produced ($R_p > 0$) or consumed ($R_p < 0$) by reactions inside the sphere during unit time. These equations represent the Gibbs–Duhem constraints on the chemical potential gradients by the p − 1 matrix minerals. The next n equations in Figure 2 are obtained by rearranging equation 11 to have the following form:

$$-\nu_{ip} = \left(4\pi x^2 \sum_{j=1}^{n} L_{ij}(\nabla\mu_j)_x + \sum_{k=1}^{p-1} \nu_{ik} R_k\right) 1/R_p$$

$$= \sum_{j=1}^{n} L_{ij} (\nabla\mu_j)_x (A/R_p) + \sum_{k=1}^{p-1} \nu_{ik} (R_k/R_p) \qquad (13)$$

$$(i=1,2,\ldots,n)$$

where $R_k = 4\pi \int_0^x J_k^i x^2 \, dx$.

These equations represent the conservation constraints which require the amount of material that diffuses into (or out of) the segregation to be used up (or produced) by the reactions taking place within the segregation. Providing the L_{ij}, ν_{ik}, and ν_i^k are known, the equation in Figure 2 can be solved using matrix algebra to obtain the relative reaction coefficients (R_k/R_p) and $(\nabla\mu_j)_x \cdot A/R_p$ terms. The latter numbers can be used to obtain ratios of the chemical potential gradients because they contain the common term A/R_p. The ν_i^k and ν_{ik} required to solve the equation in Figure 2 can be obtained from microprobe analyses of minerals in the rock to be modelled. Estimates of the appropriate phenomenological coefficients are more difficult to obtain but their relative values can be calculated under certain circumstances as explained in the following section.

$$\begin{pmatrix}
\nu_1^1 & \nu_2^1 & \nu_3^1 & \cdots & \nu_n^1 & 0 & 0 & 0 & \cdots & 0 \\
\nu_1^2 & \nu_2^2 & \nu_3^2 & \cdots & \nu_n^2 & 0 & 0 & 0 & \cdots & 0 \\
\nu_1^3 & \nu_2^3 & \nu_3^3 & \cdots & \nu_n^3 & 0 & 0 & 0 & \cdots & 0 \\
\vdots & & & & \vdots & & & & & \vdots \\
\nu_n^{p-1} & \nu_n^{p-1} & \nu_n^{p-1} & \cdots & \nu_n^{p-1} & 0 & 0 & 0 & \cdots & 0 \\
L_{11} & L_{12} & L_{13} & \cdots & L_{1n} & \nu_{11} & \nu_{12} & \nu_{13} & \cdots & \nu_{1\,p-1} \\
L_{21} & L_{22} & L_{23} & \cdots & L_{2n} & \nu_{21} & \nu_{22} & \nu_{23} & \cdots & \nu_{2\,p-1} \\
L_{31} & L_{32} & L_{33} & \cdots & L_{3n} & \nu_{31} & \nu_{32} & \nu_{33} & \cdots & \nu_{3\,p-1} \\
\vdots & & & & \vdots & & & & & \vdots \\
L_{n1} & L_{n2} & L_{n3} & \cdots & L_{nn} & \nu_{n1} & \nu_{n2} & \nu_{n3} & \cdots & \nu_{n\,p-1}
\end{pmatrix}
\cdot
\begin{pmatrix}
(\nabla\mu_1)_x \cdot A/R_p \\
(\nabla\mu_2)_x \cdot A/R_p \\
(\nabla\mu_3)_x \cdot A/R_p \\
\vdots \\
(\nabla\mu_n)_x \cdot A/R_p \\
R_1/R_p \\
R_2/R_p \\
R_3/R_p \\
\vdots \\
R_{p-1}/R_p
\end{pmatrix}
=
\begin{pmatrix}
0 \\ 0 \\ 0 \\ \vdots \\ 0 \\ -\nu_{1p} \\ -\nu_{2p} \\ -\nu_{3p} \\ \vdots \\ -\nu_{np}
\end{pmatrix}$$

Fig. 2. Matrix equations to solve for relative chemical potential gradients in the matrix surrounding a segregation and the relative reaction taking place within the segregation.

Phenomenological coefficients

Reference frame

The flow of material from one area of a rock to another must be measured by comparing the motion to some reference frame in the rock. A number of commonly used reference frames have been reviewed by Brady (1975). I prefer an inert marker reference frame because it corresponds to the intuitive view of diffusion of many petrologists. Unfortunately, the Rangeley rocks do not have a set of evenly distributed inert markers against which to measure diffusive fluxes. However, because all domains of the rocks contain quartz and the rocks were not under a deviatoric stress during the growth of mineral segregations (Guidotti, 1968; Foster, 1977a), the chemical potential of SiO_2 should be fixed throughout the rock at a given pressure and temperature. This means that if cross terms in the inert marker phenomenological coefficients involving silica are not important, the silica-fixed frame should be equivalent to the inert marker frame for these rocks. This can be verified by examining the velocity of the silica-fixed frame with respect to the boundary between the staurolite pseudomorph and the matrix surrounding it. Although the modes change at this boundary, the phases in the pseudomorph are the same as the phases in the matrix (Foster, 1977a), which indicates this boundary is passive marker (Joesten, 1977). If the silica-fixed frame is equivalent to the inert marker frame the transport of SiO_2 across this boundary should be zero. Examination of Figure 3 shows that, as expected, there is no significant difference between the silica-fixed reference frame and the inert marker reference frame in the vicinity of the staurolite pseudomorphs in rocks from the middle part of the lower sillimanite zone on Elephant Mountain. Because of the lack of other inert markers there is no direct proof that this is true in other parts of the rock. However, SiO_2 should behave as an inert marker everywhere in the rock because of the presence of quartz in all domains.

Calculation of L matrix

The minerals involved in the reactions forming the segregations shown in Figure 1 can be represented by the nine-component system FeO, MgO, $NaO_{0.5}$, CaO, TiO_2, $KO_{0.5}$, SiO_2, H_2O, $AlO_{1.5}$. MnO and ZnO have been ignored because they are important only in incongruent reactions involving garnet and staurolite respectively (Foster, 1975, 1977a). To solve the equations shown in Figure 2 for this system a maximum of 81 L_{ij} must be known. To reduce the number of phenomenological coefficients to a more manageable number I assume that, to a first approximation, the non-diagonal terms in the L matrix are zero. In addition, quartz is present throughout the rock, fixing μ_{SiO_2} and eliminating the need to know $L_{SiO_2SiO_2}$ because $L_{SiO_2SiO_2} \nabla\mu_{SiO_2} = 0$. I also assume that μ_{H_2O} is constant; the rock should be saturated with a water-

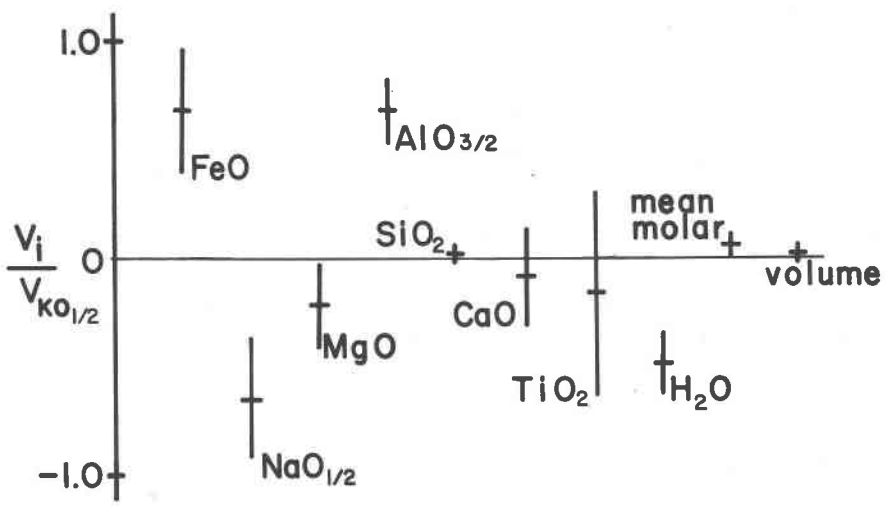

Fig. 3. Velocity ratios of some reference frames relative to the staurolite pseudomorph boundary from middle of lower sillimanite zone. Calculated using the equation for relative velocity of reference frames given in Fisher (1977, p. 394) and matrix fluxes computed using mineral compositions, modes, and net volume changes in the staurolite segregations for specimens from outcrop RA66 reported by Foster (1977a, Fig. 3, Tables 1–6, and Table 8). Vertical axis is the ratio of velocity of reference frame i to velocity of $KO_{0.5}$ reference frame. Horizontal line is mean of seven specimens. Vertical line gives one standard deviation.

rich fluid because the overall reaction is a dehydration reaction (Guidotti, 1970, 1974; Foster, 1977a). Thus, only seven L_{ij} are needed to solve the equations shown in Figure 2. Although the relative values of the phenomenological coefficients in an inert marker reference frame are a function of the composition of the fluid or grain boundary phase (Katchalsky and Curran, 1965), they can, to a first approximation, be treated as constants if the variation in composition is small. This approximation should be valid in the Rangeley rocks because the system is believed to be close to equilibrium. In addition, no systematic variation in the modes of matrix phases has been observed between segregations in these rocks. This indicates that the amount of internal precipitation (Frantz and Mao, 1976) is small, as expected in a system with nearly constant relative phenomenological coefficients. Using this approximation, the relative values of the seven remaining phenomenological coefficients can be obtained in the following manner. The fluxes in the matrix around staurolite and sillimanite segregations are constrained by the Gibbs–Duhem equations of the matrix phases. The presence of quartz and the water-rich grain boundary phase fix the chemical potentials of SiO_2 and H_2O while the two micas, plagioclase, and ilmenite provide a set of four Gibbs–Duhem relations which restrict the chemical potential gradients around each segregation. Because the cross terms in the L matrix have been neglected, each of the seven non-zero chemical potential gradients in the matrix is related to the corresponding flux by:

$$\nabla\mu_i^a = J_i^a/L_{ii} \qquad (i=1,2,\ldots,7) \tag{14}$$

where $\nabla\mu_i^a$ is the chemical potential gradient of component i in the matrix around segregation a and J_i^a is the flux of i away from segregation a. Equation 14 can be substituted into the four Gibbs–Duhem equations of the matrix phases around the staurolite and sillimanite segregations, giving a set of eight independent equations which relate the fluxes and phenomenological coefficients in a rock:

$$\sum_{i=1}^{7} \nu_i^k J_i^a/L_{ii} = 0 \qquad (k=1,2,\ldots,4;\ a=1,2) \tag{15}$$

The integral of J_i^a over a closed surface surrounding a segregation is related to the net reaction inside of segregation a during unit time by:

$$\int_s J_i^a \cdot dA = \sum_{j=1}^{5} \nu_i^j N_j^a \qquad (i=1,2,\ldots,7) \tag{16}$$

where N_j^a is the amount of phase j which reacts in segregation a and ν_i^j is the amount of component i in phase j. Integration of the J_i^a in equation 15 over a closed surface surrounding the segregation permits substitution for $\int_s J_i^a \cdot dA$ using equation 16, which gives a relationship between the reactions in a segregation and the diagonal terms of the L matrix:

$$\sum_{i=1}^{7} \nu_i^k \left[\sum_{j=1}^{5} \nu_i^j (N_j^a/L_{ii}) \right] = 0$$
$$(k=1,2,\ldots,4;\ a=1,2) \tag{17}$$

The N_j^a in equation 17 for staurolite and sillimanite segregations in each of five rocks from outcrop RA66 in the middle of the lower sillimanite zone on Elephant Mountain were calculated from the mode, volume, and composition data in Foster (1977a). For convenience, unit area was chosen to be the area of the surfaces surrounding sillimanite segregations containing one mole of sillimanite and unit time was chosen to be the time during which sillimanite grew in these rocks. The N_j^a obtained from the rocks can then be used to constrain the N_j^a/L_{ii} terms in equation 17 through equations of the form:

$$(N_j^a/L_{ii})\ 1/N_j^a - (1/L_{ii}) = 0$$
$$(i=1,2,\ldots,7;\ j=1,2,\ldots,5;\ a=1,2) \tag{18}$$

where the terms in parentheses are the unknowns. For the system shown in Figure 1 there are four equations like 17 for the staurolite segregation and four for the sillimanite segregation, making a total of eight linearly independent equations of this type per rock. In addition, there are a total of 35 equations like 18 for each segregation, giving a total of 70 linearly independent equations of this type in each rock. This system of equations cannot be solved unless one of the (N_j/L_{ii}) terms or $(1/L_{ii})$ terms is known. None of these terms are known, so the system of equations can only be solved for relative phenomenological coefficients. This is accomplished by multiplying equations 17 and 18 by one of the L_{ii} unknowns, in this case $L_{KO_{0.5}}$,[1] to produce equations of the form:

$$\sum_{i=1}^{7} \nu_i^k \sum_{j=1}^{5} \nu_i^j (N_j^a\, L_{KO_{0.5}}/L_{ii}) = 0$$
$$(k=1,2,3,4;\ a=1,2) \tag{19}$$

[1] $KO_{0.5}$ was chosen for normalization because it has large fluxes which are computed from modal data with good point-counting statistics.

and

$$(N_j^a L_{KO_{0.5}}/L_{ii})\ 1/N_j^a - ({}^LKO_{0.5}/L_{ii}) = 0$$
$$(i=1,2...,7;\ j=1,2,...,5;\ a=1,2) \qquad (20)$$

Note that when i is $KO_{0.5}$ the phenomenological coefficient ratio in equation 20 equals one, permitting a solution to be obtained if the number of equations is equal to or exceeds the number of unknowns. There are a total of 78 independent equations like 19 and 20 that constrain 76 unknowns in each rock. Thus, the system is over-determined, permitting a solution to be obtained by least-square techniques. Because the L_{ii} should be non-negative (Katchalsky and Curran, 1965), the equations were solved using a least-squares fit program (NNLS) described by Lawson and Hanson (1974, p. 269–271) which permitted the signs of the unknowns to be specified. The equations were scaled and weighted using methods in Draper and Smith (1966, p. 77–81, 145–150). The variances of the N_j^a used to calculate the weights of equations 20 were determined by propagating the standard deviations of the modes from Foster (1977a) through the calculation of the N_j^a. Thus, the equations with the most reliable N_j^a were weighted most heavily in the least-squares fit. This procedure gives the set of positive phenomenological coefficients that best fits the observed data.

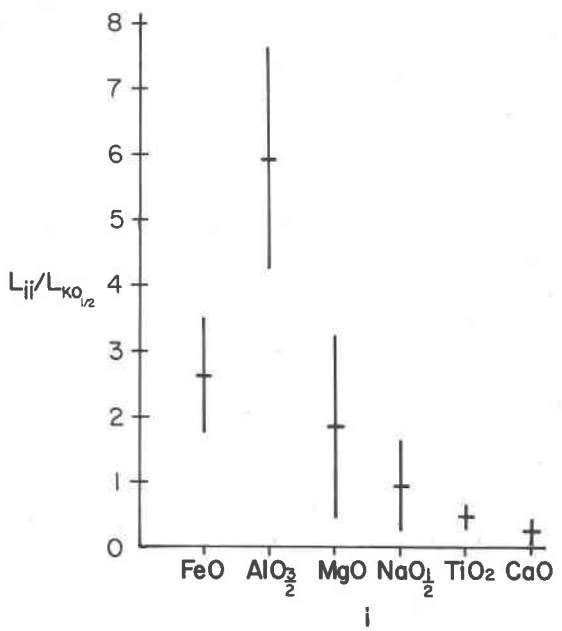

Fig. 4. Relative phenomenological coefficients in rocks from the middle of the lower sillimanite zone. Reference frame is SiO_2. It should be equivalent to inert marker frame. Horizontal line gives mean of five rocks. Vertical line gives standard deviation.

The mean and standard deviation of relative phenomenological coefficients calculated in this manner from five rocks from the middle of the lower sillimanite zone are given in Figure 4. Specimens from the middle part of the lower sillimanite zone were chosen for the analysis because the staurolite porphyroblasts have not been completely pseudomorphed in these rocks, so that the composition of both the products and reactants in the segregations can be obtained for each rock. The five specimens at outcrop RA66 were selected because they have the largest and most abundant segregations at this outcrop, which permits the best estimates of the modes in the staurolite and sillimanite segregations. An independent check of the validity of these coefficients will be discussed later.

Calculation of local reactions and chemical potential gradients

The mean values of the diagonal coefficients of the L matrix given in Figure 4 can be used in the system of equations shown in Figure 2 to theoretically predict local reactions and chemical potential gradients in the system shown in Figure 1. The three segregations form separate local systems which communicate with each other *via* material transport through the matrix. The local systems will first be considered one at a time and then assembled in a system which describes the interaction between the segregations during metamorphism. The mineral compositions, modes, and segregation volumes reported by Foster (1977a, Fig. 3, Tables 1–6 and 8) for one representative rock (RA66N) in the lower sillimanite zone will be used to illustrate the following discussion. I assume that the system is always in local equilibrium, that it is open to a water-rich fluid which fixes μ_{H_2O}, and that the mineral compositions and relative phenomenological coefficient ratios do not change during the growth of the segregations.

Sillimanite segregation

This segregation is formed when sillimanite nucleates and begins to grow in a biotite, muscovite, plagioclase, quartz, ilmenite matrix. The overall reaction which takes place between the matrix minerals and the growing sillimanite can be calculated by solving the system of equations given in Figure 5. The first four rows represent the respective Gibbs–Duhem equations for biotite, muscovite, plagioclase, and ilmenite in the matrix of RA66N. The components SiO_2 and H_2O are not included in the Gibbs–Duhem relations because their chemical po-

Table 1. Summary of symbols

A	The area of a sphere which surrounds a segregation. Superscripts s, st, and g in equations 22-24 stand for sillimanite, staurolite, and garnet segregations, respectfully.
A_m	The affinity of reaction m.
c_i	The concentration of component i in the fluid or grainboundary phase.
J_i	The flux of component i.
J_i^a	The flux of component i in the matrix around segregation a. Superscripts s, st, and g stand for sillimanite, staurolite, and garnet segregations, respectively.
J_k^r	The rate of chemical reaction k.
L_{ij}	The diffusion phenomenological coefficient which relates the flux of component i to the chemical potential gradient of component j.
$L_{KO_{0.5}}$	The phenomenological coefficient which relates the flux of $KO_{0.5}$ to the chemical potential gradient of $KO_{0.5}$.
L_{km}^r	The reaction phenomenological coefficient relating the rate of reaction k to the affinity of reaction m.
n	The number of components in the system.
N_j^a	The number of moles of mineral j in segregation a which take part in the net reaction within the segregation during the growth of one mole of sillimanite in the rock.
p	The number of solid phases in the system.
q	The number of reactions in the system.
R_k	The stoichiometric coefficient of phase k for the net reaction within a volume of rock. The subscript p stands for the core mineral in the center of a segregation which is not present in the matrix around the segregation. The subscripts s, st, and g stand for the core minerals sillimanite, staurolite, and garnet respectively.
t	Time.
V	A volume of rock surrounded by a closed surface.
x	Distance from the center of a segregation.
μ_i	The chemical potential of component i.
$\nabla\mu_i$	The chemical potential gradient of component i.
$\nabla\mu_i^a$	The chemical potential gradient of component i in the matrix around segregation a. Superscripts s, st, and g stand for sillimanite, staurolite, and garnet segregations, respectively.
$(\nabla\mu_i)_x$	The chemical potential gradient of component i evaluated at a distance x from the center of a segregation.
ν_{ik}	The stoichiometric coefficient of component i in reaction k.
ν_i^k	The stoichiometric coefficient of component i in mineral k.
$\int_V$	Integral over the volume V.
$\int_S$	Integral over a closed surface.

tential gradients are fixed at zero by the presence of quartz and the water-rich grain boundary phase in all domains. The next seven equations are the conservation relations for FeO, $NaO_{0.5}$, MgO, $AlO_{1.5}$, $KO_{0.5}$, CaO, and TiO_2, respectively. The last two equations represent conservation equations for SiO_2 and H_2O, respectively. These two equations are used to calculate the amounts of quartz and water that take part in the reaction.

The solution of these equations is given in Table 2. The net reaction among the solid phases in this segregation which produces one mole of sillimanite is:

0.28 muscovite + 0.05 plagioclase + 0.01 ilmenite →
1.0 sillimanite + 0.06 biotite + 0.52 quartz (A)

This reaction consumes three matrix phases: muscovite, plagioclase, and ilmenite. Provided that the matrix is homogeneous and the grain size is small relative to the segregation diameter, the reaction will entirely use up one of these phases in the vicinity of the growing sillimanite. In the case of RA66N, which has a matrix composed of 31% biotite, 26% muscovite, 8% plagioclase, 2% ilmenite, and 33% quartz, the muscovite will disappear before either the plagioclase or ilmenite, because reaction A consumes 1.7 mm^3 of plagioclase and 0.2 mm^3 of ilmenite for every 26 mm^3 of muscovite consumed. Thus, when the muscovite in 100 mm^3 of matrix in RA66N is used up by reaction A 6.3 mm^3 of plagioclase and 1.8 mm^3 of ilmenite remains.

Once the matrix muscovite has disappeared around the growing sillimanite, the reaction inside the muscovite-free rim surrounding the sillimanite is constrained by the Gibbs–Duhem equations of the remaining matrix phases: ilmenite, plagioclase, biotite, and quartz. To calculate the relative chemical potential gradients in the muscovite-free rim and the net reaction in that part of the segregation inside of the muscovite-free rim, the muscovite terms in the conservation equations and the muscovite reaction coefficient are removed from the matrices in Figure 5. This is accomplished by deleting row two from the square matrix and right-hand side column matrix, column nine from the square matrix, and the R_m/R_s term in the left-hand side column matrix. Because one equation and one unknown have been removed, the solution can be obtained in the manner previously described. The reaction occurring inside the muscovite-free rim to produce one mole of sillimanite is:

0.11 biotite + 0.28 plagioclase →
1.0 sillimanite + 0.37 quartz + 0.03 ilmenite (B)

The relative chemical potential terms in the muscovite-free mantle are given in Table 2. Because reactions A and B are not the same there must be a reaction at the matrix/muscovite-free mantle boundary. The reaction coefficients at this boundary

$$\begin{bmatrix}
\nu_1^B & \nu_2^B & \nu_3^B & \nu_4^B & \nu_5^B & \nu_6^B & \nu_7^B & 0 & 0 & 0 & 0 & 0 & 0 \\
\nu_1^M & \nu_2^M & \nu_3^M & \nu_4^M & \nu_5^M & \nu_6^M & \nu_7^M & 0 & 0 & 0 & 0 & 0 & 0 \\
\nu_1^P & \nu_2^P & \nu_3^P & \nu_4^P & \nu_5^P & \nu_6^P & \nu_7^P & 0 & 0 & 0 & 0 & 0 & 0 \\
\nu_1^I & \nu_2^I & \nu_3^I & \nu_4^I & \nu_5^I & \nu_6^I & \nu_7^I & 0 & 0 & 0 & 0 & 0 & 0 \\
L_{11} & 0 & 0 & 0 & 0 & 0 & 0 & \nu_{1B} & \nu_{1M} & \nu_{1P} & \nu_{1I} & 0 & 0 \\
0 & L_{22} & 0 & 0 & 0 & 0 & 0 & \nu_{2B} & \nu_{2M} & \nu_{2P} & \nu_{2I} & 0 & 0 \\
0 & 0 & L_{33} & 0 & 0 & 0 & 0 & \nu_{3B} & \nu_{3M} & \nu_{3P} & \nu_{3I} & 0 & 0 \\
0 & 0 & 0 & L_{44} & 0 & 0 & 0 & \nu_{4B} & \nu_{4M} & \nu_{4P} & \nu_{4I} & 0 & 0 \\
0 & 0 & 0 & 0 & L_{55} & 0 & 0 & \nu_{5B} & \nu_{5M} & \nu_{5P} & \nu_{5I} & 0 & 0 \\
0 & 0 & 0 & 0 & 0 & L_{66} & 0 & \nu_{6B} & \nu_{6M} & \nu_{6P} & \nu_{6I} & 0 & 0 \\
0 & 0 & 0 & 0 & 0 & 0 & L_{77} & \nu_{7B} & \nu_{7M} & \nu_{7P} & \nu_{7I} & 0 & 0 \\
0 & 0 & 0 & 0 & 0 & 0 & 0 & \nu_{8B} & \nu_{8M} & \nu_{8P} & \nu_{8I} & \nu_{8Q} & \nu_{8W} \\
0 & 0 & 0 & 0 & 0 & 0 & 0 & \nu_{9B} & \nu_{9M} & \nu_{9P} & \nu_{9I} & \nu_{9Q} & \nu_{9W}
\end{bmatrix}
\cdot
\begin{bmatrix}
(\nabla\mu_1)_x \cdot A/R_s \\
(\nabla\mu_2)_x \cdot A/R_s \\
(\nabla\mu_3)_x \cdot A/R_s \\
(\nabla\mu_4)_x \cdot A/R_s \\
(\nabla\mu_5)_x \cdot A/R_s \\
(\nabla\mu_6)_x \cdot A/R_s \\
(\nabla\mu_7)_x \cdot A/R_s \\
R_B/R_s \\
R_M/R_s \\
R_P/R_s \\
R_I/R_s \\
R_Q/R_s \\
R_W/R_s
\end{bmatrix}
=
\begin{bmatrix}
0 \\ 0 \\ 0 \\ 0 \\ -\nu_{1s} \\ -\nu_{2s} \\ -\nu_{3s} \\ -\nu_{4s} \\ -\nu_{5s} \\ -\nu_{6s} \\ -\nu_{7s} \\ -\nu_{8s} \\ -\nu_{9s}
\end{bmatrix}$$

Fig. 5. Matrix equations to solve for chemical potential gradients in matrix around sillimanite segregation and net reaction within the segregation. Solution for RA66N is given in the first column of Table 2. B, M, P, I, Q, W, S stand for biotite, muscovite, plagioclase, ilmenite, quartz, water, and sillimanite respectively. Components 1, 2, 3, 4, 5, 6, 7, 8, 9 are FeO, $NaO_{0.5}$, MgO, $AlO_{1.5}$, $KO_{0.5}$, CaO, TiO_2, SiO_2, and H_2O respectively.

can be obtained by subtracting reaction B from reaction A. It is:

0.28 muscovite + 0.04 ilmenite →

0.17 biotite + 0.23 plagioclase + 0.15 quartz (C)

The composition of the muscovite-free rim can be determined by calculating the number of moles of each phase contained in the amount of matrix needed to supply 0.28 moles of muscovite and then subtracting the number of moles of reactants and adding the number of moles of product phases in reaction C. The modes of each phase in the muscovite-free rim can be calculated by using molar volumes of the minerals to convert the mole fraction of each phase to volume percent. The modes calculated for the muscovite-free rim for RA66N are given in Figure 6a. These modes can be used with reaction B to determine if the reaction inside the muscovite-free rim will consume biotite or plagioclase first. In the case of RA66N the plagioclase is eliminated before biotite, creating a plagioclase–muscovite-free mantle around the growing sillimanite. The reaction inside this mantle can be calculated by removing the muscovite and the plagioclase terms in the matrices given in Figure 5 and solving for the remaining unknowns. The solution is given in Table 2. The reaction at the boundary between the muscovite-free and muscovite–plagioclase-free zone can be computed by subtracting the reaction calculated for the portion inside the muscovite–plagioclase-free mantle from the reaction calculated for the part of the segregation inside the muscovite-free mantle. In RA66N this reaction is:

0.28 plagioclase + 0.01 ilmenite →

0.02 biotite + 0.65 quartz (D)

Reaction D can be used to calculate the composition of the muscovite–plagioclase-free mantle by subtracting or adding the reaction coefficients to the amount of muscovite-free mantle which contains 0.28 moles of plagioclase.

The reaction inside the muscovite–plagioclase-free mantle (Table 2) will consume biotite in RA66N before it consumes quartz, creating a quartz + ilmenite mantle next to the growing sillimanite. The reaction between the biotite-bearing mantle and the biotite-free mantle is given in Figure 6a. It was calculated by subtracting the reaction for the segregation inside the biotite-free rim from the reaction inside the muscovite–plagioclase-free rim (Table 2). The modes of the biotite-free mantle were calculated from the interface reaction and modes of the muscovite–plagioclase-free mantle in the same manner as for the other mantles. The biotite-free mantle is converted into the sillimanite–ilmenite core by a reaction that consumes quartz and produces sillimanite (Table 2 and Fig. 6). It does not involve ilmenite because, when the biotite disappears, ilmenite is the only Fe- and Ti-bearing mineral in the interior of the segregation. To dissolve or precipitate ilmenite in this part of the segregation

Table 2. Chemical potential gradients and net reactions within segregations (calculated)

$(\nabla\mu_i)_x \cdot A/R_p$**

	Sillimanite* Segregation				Staurolite Segregation	Garnet* Segregation				
i	Matrix	(M)	(MP)	(MPB)	Matrix	Matrix	(B)	(BP)	(BPI)	(BPIM)
FeO	0.05	-0.09	-0.11	0.0	0.83	0.39	0.82	0.82	0.93	0.94
$NaO_{0.5}$	-0.14	-0.24	-0.01	0.0	-1.25	-0.26	-0.23	-0.09	-0.09	0.0
MgO	0.05	-0.11	-0.14	0.0	-0.05	-0.37	0.13	0.13	0.13	0.13
$AlO_{1.5}$	0.10	0.22	0.26	0.34	0.96	0.16	0.10	0.10	0.10	0.34
$KO_{0.5}$	-0.33	-0.18	-0.22	0.0	-3.22	-0.52	-0.34	-0.39	-0.40	0.0
CaO	-0.07	-0.36	0.0	0.0	-0.94	0.03	0.27	0.51	0.51	0.51
TiO_2	-0.05	0.09	0.11	0.0	-0.81	-0.38	-0.80	-0.80	-0.03	0.0

R_j/R_p***

	Sillimanite Segregation				Staurolite Segregation	Garnet Segregation				
j	Matrix	(M)	(MP)	(MPB)	Matrix	Matrix	(B)	(BP)	(BPI)	(BPIM)
B	0.06	-0.11	-0.13	-	-0.19	-0.52	-	-	-	-
M	-0.28	-	-	-	-1.84	0.22	-0.21	-0.25	-0.25	-
P	-0.05	-0.28	-	-	-0.73	-0.37	-0.18	-	-	-
I	-0.01	0.03	0.04	0.0	-0.14	-0.02	-0.15	-0.14	-	-
Q	0.52	0.38	-0.27	-1.00	6.65	-0.49	-1.15	-1.46	-1.42	-2.98
W	0.43	0.22	0.27	0.0	2.07	0.60	0.43	0.50	0.51	0.0
S	1.00	1.00	1.00	1.00	-	-	-	-	-	-
St	-	-	-	-	1.00	-	-	-	-	-
G	-	-	-	-	-	1.00	1.00	1.00	1.00	1.00

*Mantles around segregation are identified by the missing matrix phases in brackets (eg. (M) = muscovite-free mantle).

**This term gives relative chemical potential gradients in the region identified by the column heading.

***This term gives relative stoichiometric coefficients for the net reaction in the portion of the segregation enclosed by the region identified in the column heading.

would require Fe and Ti to diffuse in the same direction through the quartz + ilmenite mantle. This is prevented because of the constraint on the chemical potential gradients of Fe and Ti provided by the ilmenite Gibbs–Duhem equation. As the quartz is replaced by sillimanite, ilmenite is passed from the mantle into the core. The modes of the core region are calculated by using the core/biotite-free mantle reaction and the biotite-free mantle modes to calculate the amount of ilmenite passed into the core when one mole of quartz is converted to one mole of sillimanite.

The volumes for each mantle are calculated by subtracting the amount of mantle consumed by the local reaction on the inner margin of the mantle from the amount of mantle produced by the local reaction on the outer margin of the mantle. For example, the volume of the muscovite-free mantle can be calculated by subtracting the amount of muscovite-free rim consumed by reaction D from the amount produced by reaction C. The radius of each boundary shown in Figure 6a is calculated by adding the volumes of the portions of the segregation inside of each boundary together and calculating the radius of a sphere having this volume.

The calculated local reactions, modes, and thick-

ness of mantles in a segregation produced by the growth of one mole of sillimanite in a matrix similar to that of RA66N are given in Figure 6a. The size of the segregation depends upon the amount of sillimanite which has grown in the core of the segregation. However, the sequence of mantles, relative thickness of mantle, and modes are independent of the amount of sillimanite growth. They depend only on the mineral compositions and mode of the original matrix.

The distribution of minerals within the sillimanite segregation provides a way to test the validity of the procedures used to calculate the segregation form because the internal fluxes of the segregation were not used to calculate the relative phenomenological coefficients. In previous work (Foster, 1975, 1977a) two compositionally distinct regions in the sillimanite segregation were recognized: a dark-colored biotite-rich, muscovite-free mantle and a light-colored biotite-poor, sillimanite-rich core. The biotite-rich mantle in Foster (1977a) corresponds to the outer two mantles shown in Figure 6a while the sillimanite-rich core in Foster (1977a) combines the quartz + ilmenite mantle and the sillimanite + ilmenite core region of Figure 6a. Re-examination of the thin sections used in the 1977 work shows that the outer part of the biotite rim commonly contains most of the plagioclase while the outer part of the sillimanite core is quartz- and ilmenite-rich. This was not previously recognized because the color contrast of the segregation does not appreciably change when the mode of plagioclase and quartz varies. An additional complication is that because the primary sedimentary lamination is still present in the sillimanite-bearing rocks the matrix is not completely uniform. A local variation in the plagioclase, biotite, ilmenite, or quartz mode of the original matrix can cause the inner sequence of mantles to change. This may account for the presence of small amounts of biotite and plagioclase in the core region (Foster, 1977a, Fig. 3) and the irregular concentration of ilmenite in the core region (Foster, 1977a, p. 730). A comparison between the average modes and thicknesses of the biotite-rich rim and the biotite-poor core from specimen RA66N with the values calculated from the model sillimanite segregation shown in Figure 6 are given in Table 3. The comparison between the observed and calculated values in the segregation interior provides a fairly good independent test of the procedures and assumptions used to construct the model, because the distribution of material within the segregation was not used to derive the relative phenomenological coefficients. The close agreement between the calculated and observed values indicates that the assumptions and procedures used to calculate the model are valid.

Table 3. Comparison of calculated and observed textures for specimen RA66N

	Observed	Calculated
Sillimanite Segregation		
Core radius / Mantle radius	0.53	0.64
Core modes		
Sillimanite	83 %	62 %
Quartz	9 %	34 %
Ilmenite	2 %	4 %
Biotite	6 %	--
Mantle modes		
Biotite	45 %	52 %
Quartz	38 %	39 %
Plagioclase	3 %	8 %
Ilmenite	1 %	1 %
Sillimanite	10 %	--
Muscovite	3 %	--
Staurolite Segregation		
Pseudomorph modes		
Biotite	10 %	9 %
Muscovite	82 %	75 %
Plagioclase	1 %	11 %
Ilmenite	1 %	1 %
Quartz	6 %	4 %

Staurolite segregation

This segregation forms when staurolite poikiloblasts begin to dissolve in a biotite, muscovite, plagioclase, quartz matrix. The overall reaction which takes place between the matrix minerals and the dissolving staurolite can be calculated by replacing the sillimanite values with the appropriate staurolite composition in the right-hand matrix shown in Figure 5. Solving this equation will then give the reaction and chemical potential terms relative to the stoichiometric coefficient of staurolite. The solution is given in Table 2. The net reaction which consumes one mole of staurolite ($R_p = -1$) is:

$$\begin{aligned} 1.0 \text{ staurolite} + 6.6 \text{ quartz} \rightarrow \\ 0.2 \text{ biotite} + 1.8 \text{ muscovite} \\ + 0.7 \text{ plagioclase} + 0.1 \text{ ilmenite} \end{aligned} \qquad \text{(E)}$$

This reaction consumes staurolite and quartz in a volume ratio of 3:1. Because the amount of poikiloblastic quartz in the staurolite porphyroblast is commonly 25–30 percent, the staurolite is entirely consumed before the quartz is used up. The resulting

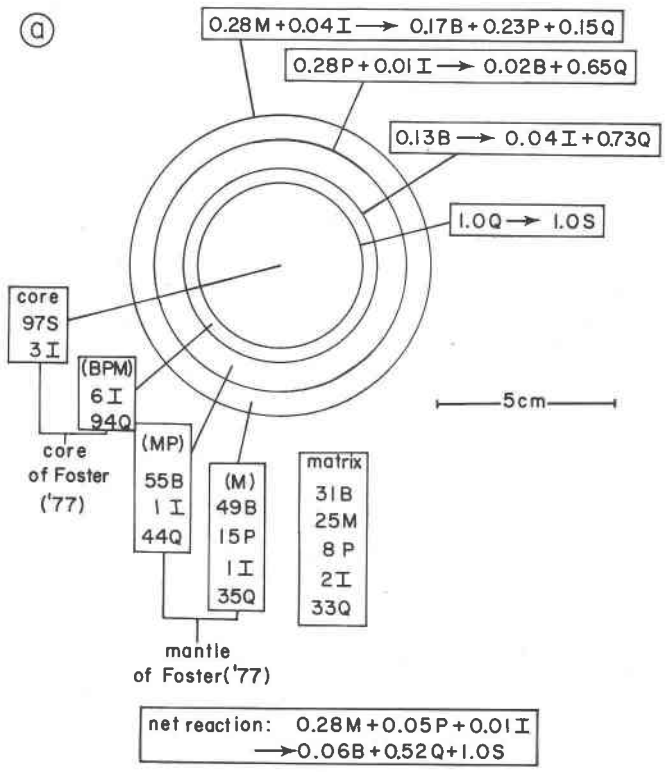

SILLIMANITE SEGREGATION

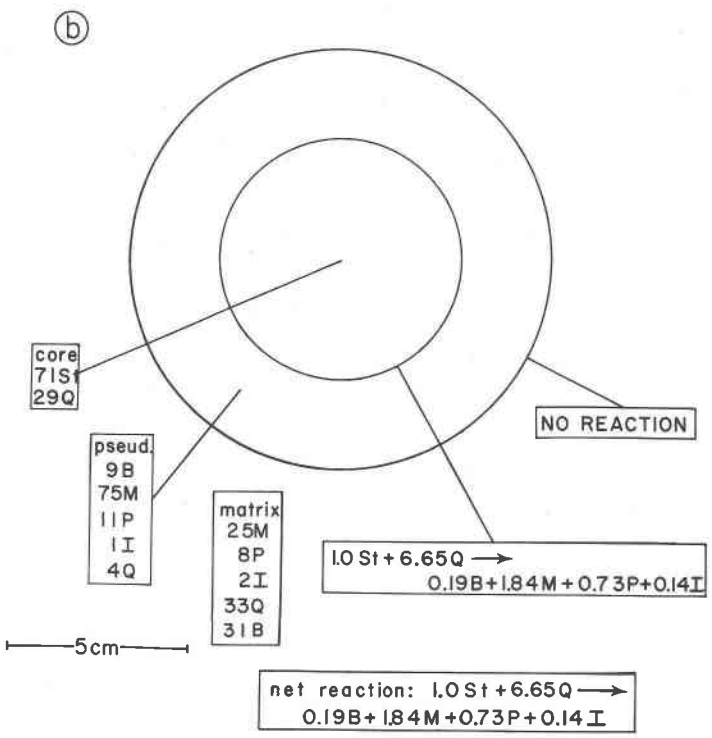

STAUROLITE SEGREGATION

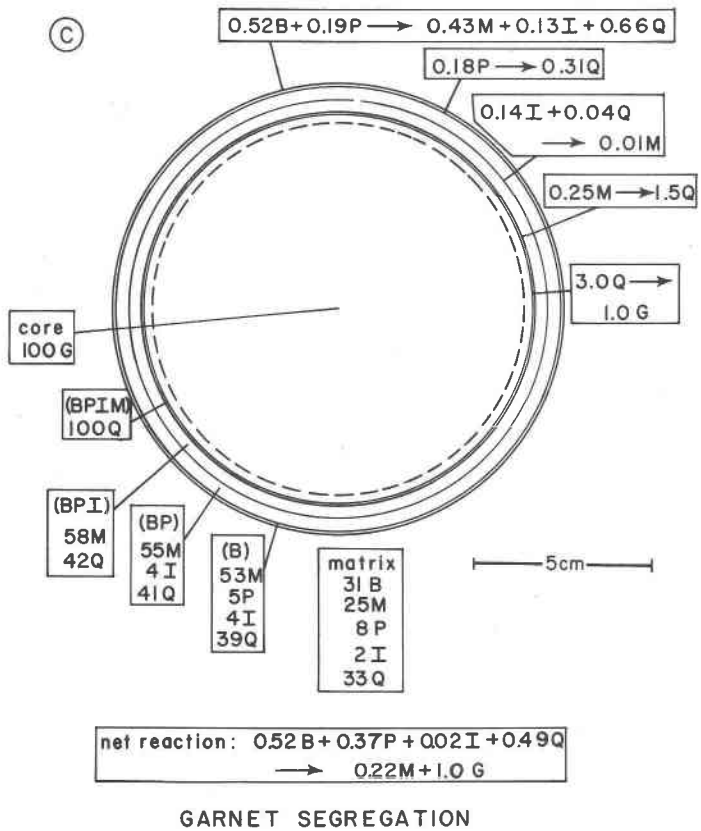

Fig. 6. Sillimanite, staurolite and garnet segregations calculated for specimen RA66N. Vertical boxes contain modes, horizontal boxes contain local reactions. Mantles are identified by absent matrix phase in parentheses [*e.g.* (M) = muscovite-free]. (a) Segregation produced by growth of one mole of sillimanite. (b) Segregation produced by pseudomorphing of one mole of staurolite. (c) Segregation produced by growth of one mole of garnet. Dashed line gives garnet boundary prior to new growth.

pseudomorph which replaces the staurolite poikiloblast consists of the biotite, muscovite, plagioclase, and ilmenite produced plus the few percent poikiloblastic quartz which was not used by reaction E. The observed and calculated modes for this segregation in rock RA66N are given in Table 3. Again, a close match is observed, but this is to be expected because the overall reaction in the staurolite segregation was used to calculate the phenomenological coefficients. The modes and local reactions are given in Figure 6b for the segregation formed when a poikiloblast originally containing 1.3 moles of staurolite is partially pseudomorphed by micas due to a reaction consuming 1.0 moles of staurolite in a matrix similar to RA66N. It can now be easily shown that the matrix/pseudomorph boundary acts as an inert marker even though the modes change: the solution to the matrix equation on either side of this boundary will always give reaction E because the same phases are present on both sides of the boundary to buffer the chemical potential gradients.

Garnet segregation

This segregation should form when garnets surrounded by a matrix of biotite, muscovite, plagioclase, quartz, and ilmenite begin to grow in a local reaction that helps balance the overall staurolite breakdown reaction for the whole rock as shown in Figure 1. The segregation for this case can be calculated by following an approach that is identical to that outlined for the sillimanite segregation except that garnet is used as the growing core mineral. The segregation predicted by the model when 1.0 mole of new garnet grows on a pre-existing porphyroblast is shown in Figure 6c. Comparison of the model garnet textures with the observed textures in the Rangeley rocks shows that in this case the match is not good. Although there is a tendency for the matrix around garnets to be plagioclase- and biotite-poor, no systematic distribution of mantles around the matrix garnets in the lower sillimanite zone has been observed. The apparent reason for the lack of mantles

around the garnets is that only a small amount of new garnet growth took place on each porphyroblast, so that the thickness of the mantles which should have formed is about the same as the size of the mica grains in the matrix around the garnets. At this scale the matrix is not homogeneous because the local composition in the vicinity of the garnet varies widely on account of the irregular distribution of individual grains. Presumably, if more garnet growth took place or if the matrix were finer-grained the calculated sequence of mantles would develop.

Whole-rock reaction

The relative amount of growth of each segregation can be calculated by the principle of mass balance, provided that an estimate of the material entering or leaving the rock on a handspecimen scale can be obtained. Because the field relations and previous studies (Guidotti, 1970, 1974; Foster, 1977a) indicate that the rocks are dehydrating as sillimanite grows, the system is assumed to be open to H_2O but closed to all other components. This means that, provided all reactions in the rock take place within the three segregations, the integrals of the fluxes of each of the seven conserved components in the matrix outside of the three segregations must sum to zero:

$$\int_s J_i^s \cdot dA^s + \int_s J_i^g \cdot dA^g + \int_s J_i^{st}\, dA^{st} = 0 \qquad (i=1,2,\ldots,7) \qquad (21)$$

After integrating and dividing through by the appropriate phenomenological coefficient this equation becomes:

$$\nabla\mu_i^s \cdot A^s + \nabla\mu_i^{st} \cdot A^{st} + \nabla\mu_i^g \cdot A^g = 0 \qquad (i=1,2,\ldots,7) \qquad (22)$$

which leads to:

$$-(\nabla\mu_i^s \cdot A^s/R_s) = (\nabla\mu_i^{st} \cdot A^{st}/R_{st})\, R_{st}/R_s + (\nabla\mu_i^g \cdot A^g/R_g)\, R_g/R_s \qquad (i=1,2,\ldots,7) \qquad (23)$$

The terms in parentheses are part of the solution of the matrix equations used to obtain the overall reaction for each segregation. They are given for each component in Table 2. The amount of staurolite and garnet which react during the growth of one mole of sillimanite can be calculated with a least-squares fit to the seven equations having the form of equation 23. The results for RA66N are $R_g/R_s = 0.08$ and $R_{st}/R_s = -0.12$. These ratios can be used to relate the reactions in the staurolite and garnet segregations to the growth of the sillimanite segregation. The results of these calculations for the growth of 0.06 mole of sillimanite in 100cm^3 rock RA66N are shown in Figure 7. Comparison with the observed textures shows that the model closely matches the staurolite and sillimanite segregations, but not the garnet segregation, which does not show distinct mantles in the rocks. As discussed previously, this is probably due to the small amount of new garnet growth and the large grain size of the matrix phases relative to the mantle thickness.

Yardley (1977) has pointed out that the absolute rate of complex ionic cycle reaction mechanisms is related to the supply of heat to the rock. In the present case, if the absolute sizes of the chemical potential gradients are too small to permit the reactions in Figure 7 to consume heat as fast as it is supplied to the rock, the temperature will rise. This will cause the absolute values of the gradients to increase as the rock moves farther from equilibrium, resulting in more rapid material transport, which increases the reaction rate. When the rate of consumption of heat by the endothermic reaction equals the rate of supply of heat, the rock will reach a steady state and the temperature and reaction rate will remain constant. On the other hand, if the absolute size of the gradients permit the endothermic reaction to use heat more rapidly than it is supplied to the rock, the temperature will fall, decreasing the chemical potential gradients until the reaction consumes the same amount of heat that is supplied to the rock. Provided that local equilibrium is maintained and the whole-rock equilibrium has not been overstepped enough to permit sillimanite to nucleate directly on garnet or staurolite, the relative reactions, relative gradients, segregation morphology, and modes will be the same regardless of the absolute rate of the endothermic reaction because they are governed only by the conservation equations and Gibbs–Duhem equations of the phases present.

Chemical potential profiles

The physical processes governing material transport throughout the rock during the growth of a specific amount of sillimanite (R_s) in the lower sillimanite zone can be illustrated by constructing profiles of the chemical potential of each component along a line from one segregation to another as shown in Figure 7. These profiles are constructed by using the reaction coefficients (R_p/R_s) of the core minerals which

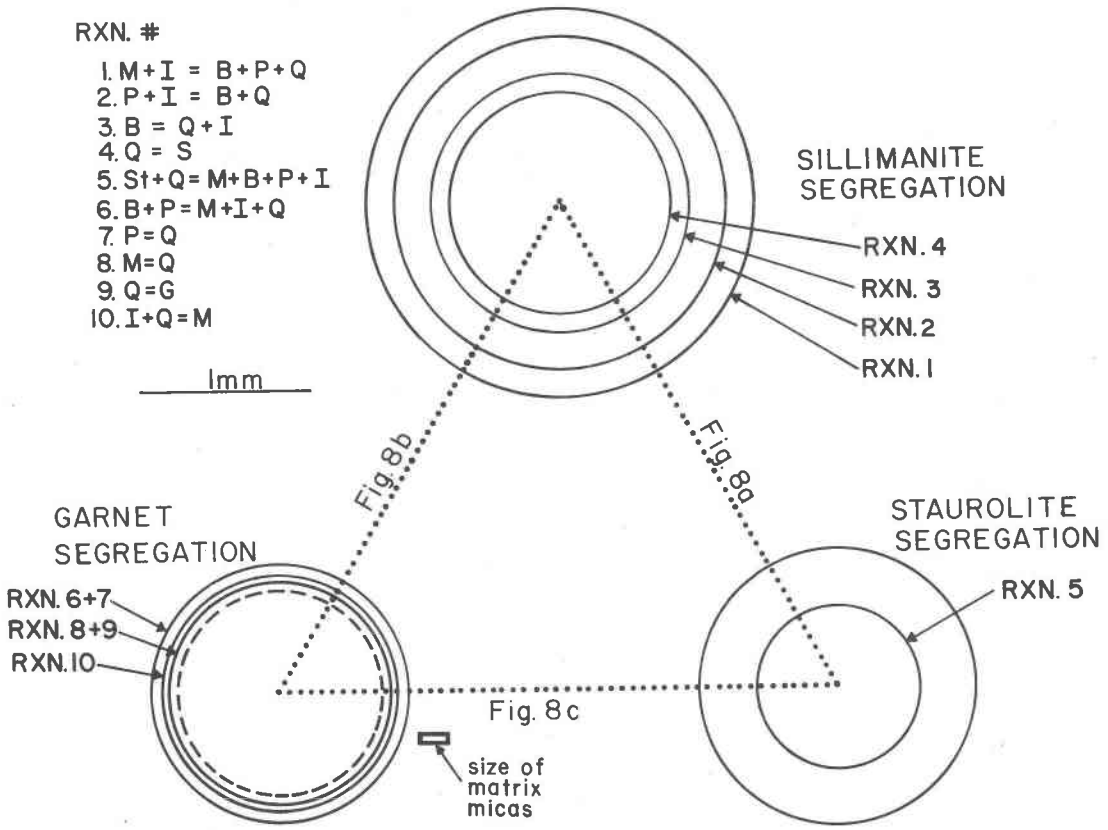

Fig. 7. Whole-rock texture with segregation spacing and size approximately equal to average segregations in RA66N. The two thinnest mantles in the garnet segregation were not shown because of reduced size. The sillimanite segregations in 100 cm^3 of rock contain 0.06 mole of sillimanite. Dotted lines show profile positions for Fig. 8.

were calculated in the previous section and the chemical potential terms $[(\nabla\mu_i)_x \cdot A/R_p]$ given in Table 2. The relative value of the gradient at a distance x from the center of each of the segregations shown in Figure 7 is given by:

$$[(\nabla\mu_i)_x/R_s] = [(\nabla\mu_i)_x \cdot A/R_p] \cdot (R_p/R_s) \cdot (4\pi x^2)^{-1} \quad (24)$$
$$(p=s, st, g;\ R_s=\text{constant})$$

where the term $4\pi x^2$ is the area (A) of the surface of a sphere with radius x surrounding the segregation. Because the value of R_s is a constant, these gradients can then be integrated from the center of one segregation to another, giving the relative value of the chemical potentials along the profile lines shown in Figure 7. Because only relative gradients are known, the standard state for all components was chosen to be the value at the center of the sillimanite segregation. The difference between $\mu_{KO_{0.5}}$ in the center of the staurolite segregation and the standard state was chosen to have unit value. The profiles shown in Figure 8 provide an interesting view of the interplay between the local reactions and chemical potential gradients in the rock, and their effect on the material transport. Reactions which are sources for a component produce discontinuities which form a ridge on the chemical potential profile while reactions which are sinks are marked by discontinuities which form a depression on the profile. If the profile crosses a reaction interface with little or no discontinuity, it is not an important source or sink for that component. The sources, sinks, and direction of transport of all components in all parts of the rock can be determined from the chemical potential profiles. For example, consider Al. One of the two major sources for transported Al in the rock is the staurolite breakdown reaction at the porphyroblast/pseudomorph boundary within the staurolite segregation. This reaction produces Al that diffuses away from the staurolite segregation due to the steep $\mu_{AlO_{1.5}}$ gradient in the pseudomorph and matrix. The other major Al source in the rock is the breakdown of muscovite at the outer boundary of the sillimanite segregation. The gradient steepens when it crosses from the matrix to the muscovite-free mantle because the Al pro-

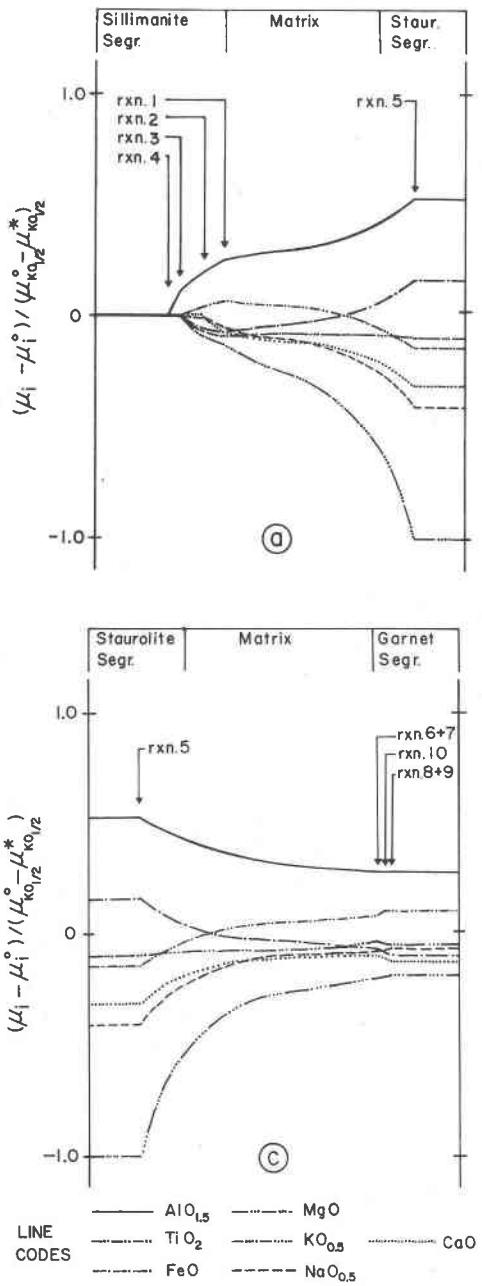

Fig. 8. Relative chemical potential profiles between segregations. The term μ_i° is the chemical potential of component i in the core of the sillimanite segregation and $\mu^*_{KO_{0.5}}$ is the chemical potential of $KO_{0.5}$ in the core of the staurolite segregation. Note that the curvature of the chemical potential profiles between reaction sites is due to the x^{-2} term in equation 24, not internal precipitation.

duced from the muscovite breakdown reaction must be transported away as well as the Al supplied by diffusion through the matrix from the dissolving staurolite. The major Al sink in the rock is provided by the growth of sillimanite at the core/mantle boundary of the sillimanite segregation.

Conclusions

The results show that textures commonly observed in pelites from the lower sillimanite zone on Elephant Mountain near Rangeley, Maine can be explained by an irreversible thermodynamic model. Preliminary studies (Foster, 1977b,c, 1978, 1980, and unpublished data) of other textures from amphibolite-facies pelites suggest that models of this type with similar relative phenomenological coefficients are valid for pelitic rocks throughout the amphibolite facies. If this is substantiated by future studies, irreversible thermodynamic models will become a powerful tool used to understand processes which form metamorphic segregations. Ultimately, quantitative models of segregation growth will be of considerable value in the interpretation of polymetamorphic terraines because they will permit the reconstruction of previous mineral assemblages from the textures preserved in the rock. With these data, it should then be possible to map different generations of isograds in detail by using the distribution of pseudomorphs and segregations in the field.

Acknowledgments

Portions of the work presented here were done at the Johns Hopkins University, the University of California, Los Angeles, and the University of Iowa. Support was provided by NSF grants #DES71-0408A02 (Fisher) and #EAR77-10649 (Ernst) as well as an Old Gold Faculty Fellowship at the University of Iowa. The reviews of previous drafts of this manuscript by G. W. Fisher,

S. N. Olsen, C. V. Guidotti, R. Joesten, and J. Brady are greatly appreciated.

References

Bailes, A. H. and McRitchie, W. D. (1978) The transition from low to high grade metamorphism in the Kisseynew sedimentary gneiss belt, Manitoba. In Metamorphism in the Canadian Shield, Geological Survey of Canada, Paper 78-10, 155–178.

Brady, J. B. (1975) Reference frames and diffusion coefficients. American Journal of Science, 275, 945–983.

Carmichael, D. M. (1969) On the mechanism of prograde metamorphic reactions in quartz-bearing pelitic rocks. Contributions to Mineralogy and Petrology, 20, 244–267.

DeGroot, S. R. and Mazur, P. (1962) Non-equilibrium Thermodynamics. North Holland Publishing Co., Amsterdam, The Netherlands.

Draper, N. R. and Smith, H. (1966) Applied Regression Analysis. Wiley, New York.

Eugster, H. P. (1970) Thermal and ionic equilibria among muscovite, K-feldspar and aluminosilicate assemblages. Fortschritte der Mineralogie, 47, 106–123.

Fisher, G. W. (1970) The application of ionic equilibria to metamorphic differentiation: an example. Contributions to Mineralogy and Petrology, 29, 91–103.

Fisher, G. W. (1973) Non-equilibrium thermodynamics as a model for diffusion-controlled metamorphic processes. American Journal of Science, 273, 897–924.

Fisher, G. W. (1975) The thermodynamics of diffusion-controlled metamorphic processes. In A. R. Cooper and A. H. Heuer, Eds., Mass Transport Phenomena in Ceramics, p. 111–112. Plenum, New York.

Fisher, G. W. (1977) Nonequilibrium thermodynamics in metamorphism. In D. G. Fraser, Ed., Thermodynamics in Geology, p. 381–403. Reidel, Boston.

Foster, C. T., Jr. (1975) Diffusion Controlled Growth of Metamorphic Segregations in Sillimanite Grade Pelitic Rocks Near Rangeley, Maine, U.S.A. Ph.D. Thesis, The Johns Hopkins University, Baltimore, Maryland.

Foster, C. T., Jr. (1976) Diffusion-controlled growth of sillimanite segregations. (abstr.) Geological Society of America Abstracts with Programs, 8, 873.

Foster, C. T., Jr. (1977a) Mass transfer in sillimanite-bearing pelitic schists near Rangeley, Maine. American Mineralogist, 62, 727–746.

Foster, C. T., Jr. (1977b) Staurolite pseudomorph textures. (abstr.) Geological Society of America Abstracts with Programs, 9, 979.

Foster, C. T., Jr. (1977c) Thermodynamic control of the migration of components in a pelitic schist. (abstr.) EOS, Transactions, American Geophysical Union, 58, 1251.

Foster, C. T., Jr. (1978) Thermodynamic models of aluminum silicate reaction textures. (abstr.) Geological Society of America Abstracts with Programs, 10, 403.

Foster, C. T., Jr. (1980) A thermodynamic model of a sillimanite/garnet texture. (abstr.) EOS, Transactions, American Geophysical Union, 61, 389.

Frantz, J. D. and Mao, H. K. (1976) Bimetasomatism resulting from intergranular diffusion: I. A theoretical model for monomineralic reaction zone sequences. American Journal of Science, 276, 817–840.

Frantz, J. D. and Mao, H. K. (1979) Bimetasomatism resulting from intergranular diffusion: II. Prediction of multimineralic zone sequences. American Journal of Science, 279, 302–323.

Guidotti, C. V. (1968) Prograde muscovite pseudomorphs after staurolite in the Rangeley–Oquossoc area, Maine. American Mineralogist, 53, 1368–1376.

Guidotti, C. V. (1970) The mineralogy and petrology of the transition from the lower to upper sillimanite zone in the Oquossoc area, Maine. Journal of Petrology, 11, 277–336.

Guidotti, C. V. (1974) Transition from staurolite to sillimanite zone, Rangeley quadrangle, Maine. Geological Society of America Bulletin, 85, 475–490.

Hollister, L. S. (1977) The reaction forming cordierite from garnet, the Khtada Lake metamorphic complex, British Columbia. Canadian Mineralogist, 15, 217–229.

Joesten, R. (1977) Evolution of mineral assemblage zoning in diffusion metasomatism. Geochimica et Cosmochimica Acta, 41, 649–670.

Katchalsky, A. and Curran, P. F. (1965) Nonequilibrium Thermodynamics in Biophysics. Harvard University Press, Cambridge, Massachusetts.

Korzhinskii, D. S. (1959) Physiochemical basis of the analysis of the paragenesis of minerals. Consultants Bureau, New York.

Lawson, C. L. and Hanson, R. J. (1974) Solving Least Squares Problems. Prentice Hall, Englewood Cliffs, New Jersey.

Loomis, T. P. (1976) Irreversible reactions in high-grade metapelitic rocks. Journal of Petrology, 17, 559–588.

Olsen, S. N. (1972) Petrology of the Baltimore Gneiss. Ph.D. Thesis, The Johns Hopkins University, Baltimore, Maryland.

Sokolnikoff, I. S. and Redheffer, R. M. (1966) Mathematics of Physics and Modern Engineering, second edition. McGraw-Hill, New York.

Thompson, J. B., Jr. (1959) Local equilibrium in metasomatic processes. In P. H. Abelson, Ed., Researches in Geochemistry, 1, p. 427–457. Wiley, New York.

Weare, J. H., Stephens, J. R. and Eugster, H. P. (1976) Diffusion metasomatism and mineral reaction zones: general principles and application to feldspar alteration. American Journal of Science, 276, 767–816.

Yardly, B. W. D. (1977) The nature and significance of the mechanism of sillimanite growth in the Connemara schists, Ireland. Contributions to Mineralogy and Petrology, 65, 53–58.

Manuscript received, January 2, 1980;
accepted for publication, July 24, 1980.